Local Spin III: Wave Function Analysis along a Reaction Coordinate, H Atom Abstraction, and Addition Processes of Benzyne

Aurora E. Clark and Ernest R. Davidson*

Department of Chemistry, Indiana University, Bloomington, Indiana 47405-7102

Received: April 17, 2002

The recently derived local spin operator $\langle \boldsymbol{S}_A^2 \rangle$ directly determines the spin state of an atom or molecular fragment *A*, whereas the $\langle \boldsymbol{S}_A \cdot \boldsymbol{S}_B \rangle$ operator represents the Heisenberg Hamiltonian spin coupling between A and B. Although one typically associates such spin properties with open-shell molecules, in the single-determinant molecular orbital approximation, these operators may be related to chemically relevant quantities such as bond order regardless of whether the system has unpaired electrons. Here we demonstrate the usefulness of these operators as molecular properties that can be applied to wave functions for which many properties are not defined, namely, multideterminant wave functions. Analysis of the wave functions of *o*-, *m*-, and *p*-benzyne indicates that these spin operators are able to detect subtle differences in electronic structure within a series of isomers with unpaired electrons. Hydrogen atom addition and abstraction processes are then used to illustrate that the operators are able to track changes in a wave function along a reaction coordinate and to obtain chemically relevant information about the development of radical character on an atom and the extent of spin coupling between atoms that are involved in bond formation.

Introduction

When unpaired electrons are present in a molecule, the question of whether to use a single- or multideterminant wave function is a familiar topic of debate. Aside from issues of computational expense, single-determinant wave functions such as those of Hartree−Fock (HF) theory are easier to interpret, and many conceptual properties (such as bond order and free valence) may be used to characterize the electronic structure. There are fewer properties whose definitions extend to multi-determinant wave functions such as those of valence bond (VB) theory, and frequently those that do are chemically nonintuitive. Nevertheless, if more than one unpaired electron is present in a molecule, a multideterminant description is frequently closer to the correct wave function for these systems.

Recently, we reported definitions for the $\boldsymbol{S}_A^2$ and $\boldsymbol{S}_A \cdot \boldsymbol{S}_B$ operators found in the Heisenberg Hamiltonian that is used to describe magnetic interactions between atoms with localized, singly occupied orbitals.[1] These local spin operators directly determine the spin state of an atom or molecular fragment. In the single-determinant approximation, these quantities may be related to other chemically relevant properties such as bond order. For example, in the single-determinant molecular orbital (MO) approximation, $\langle \boldsymbol{S}_A^2 \rangle$ for a closed-shell molecule is $^3/_8$ times the total number of bonds to A, and $\langle \boldsymbol{S}_A \cdot \boldsymbol{S}_B \rangle$ is $-^3/_8$ of the bond order between A and B. Thus, even in nonmagnetic systems, these spin operators are nonzero and provide information about the local electronic structure of an atom or molecular fragment. For open-shell systems, both the number of bonds and the "free valence" (or radical character) of A contribute to $\langle \boldsymbol{S}_A^2 \rangle$. Importantly, for singlet diradicals, different $\langle \boldsymbol{S}_A \cdot \boldsymbol{S}_B \rangle$ values can be expected from a delocalized MO single-determinant description [$\langle \boldsymbol{S}_A \cdot \boldsymbol{S}_B \rangle = -^3/_8$] versus a localized multideterminant VB wave function [$\langle \boldsymbol{S}_A \cdot \boldsymbol{S}_B \rangle = -^3/_4$]. One could state that the ionic contribution to the MO description decreases $\langle \boldsymbol{S}_A \cdot \boldsymbol{S}_B \rangle$ relative to that of a purely covalent VB function. Thus, a large degree of bonding between the two centers will favor the $-^3/_8$ value, whereas two noninteracting but spin-coupled centers will have $\langle \boldsymbol{S}_A \cdot \boldsymbol{S}_B \rangle$ equal to $-^3/_4$.

Herein, we continue our study of local spin operators and demonstrate their usefulness as molecular properties for multi-determinant wave functions that can (1) be chemically intuitive, (2) detect subtle differences in electronic structure for a series of isomers with unpaired electrons, and (3) track changes in a wave function along a reaction coordinate.

To investigate point (2), we examine the electronic structures of *o*-,[2] *m*-,[3] and *p*-benzyne.[4] These isomeric diradicals are important synthetic intermediates that have been fairly well characterized both theoretically and experimentally. Previously, the analysis of benzyne has focused on the radical character at each dehydrogenated C center as well as the spin-coupling interaction between the lone electrons. These attributes have been related to several quantum mechanical observables such as the vertical energy difference between the singlet ground state and the first triplet excited state (ΔE_{ST})[5] as well as the number of effectively unpaired electrons of the molecule, N_D.[6,7] Because $\boldsymbol{S}$ equal to zero spin coupling between the diradical electrons is energetically stabilizing, ΔE_{ST} is a good approximation to the relative strength of the radical coupling and, analogously, the diradical character. Direct calculation of N_D agrees with the ΔE_{ST} correlation. Thus, *o*-benzyne, which has the largest ΔE_{ST}, has the least diradical character, followed by *m*- and *p*-benzyne. Unlike the previous analyses, local spin operators provide a way to calculate the extent of the diradical spin coupling interaction directly and to determine how this phenomenon perturbs the electronic structure throughout the molecule.

To test point (3), we compare our current analysis of a potential energy surface with the results of a previous VB study that contains complementary information.[6] Specifically, we examine the H atom addition to *o*-,[2] *m*-,[3] and *p*-benzyne[4] and

* To whom correspondence should be addressed. E-mail: davidson@indiana.edu.

10.1021/jp020992q CCC: $22.00
Published on Web 06/22/2002

the corresponding H atom abstraction from methane. The prior analysis of the addition and abstraction PES determined the contribution of relevant VB functions to a full configuration interaction (FCI) wave function using a dihydrogen diradical to model benzyne. This analysis subsequently results in information about the spin pairing of the diradical electrons along the reaction coordinate. In contrast to the VB analysis, local spin operators are easily applied to the actual benzyne wave function. As in the dihydrogen diradical study, the radical centers become less antiferromagnetically coupled along the addition and abstraction PES. In the abstraction, "unpairing" of the electrons within the bond that is broken is also observed. To illustrate the versatility of these operators, we have used $\langle \boldsymbol{S}_A \cdot \boldsymbol{S}_B \rangle$ and $\langle \boldsymbol{S}_A{}^2 \rangle$ to monitor simultaneously the interactions between atoms that are involved in bond formation and dissociation as well as the development of radical character at a given center.

Computational Methods

Because we are interested in the properties of a wave function rather than the energy of the system, we have used a method that yields qualitatively correct wave functions for both the individual benzyne molecules and their respective addition and abstraction reactions. Consequently, we utilize the (n e$^-$, n orbital) complete active space self-consistent field (CASSCF) method[8−11] with the 6-31G* basis set[12] as implemented in HONDO99.[13] This method optimizes the coefficients of each configuration that participates in the wave function, so it is able to transform smoothly between a point on a reaction coordinate that is best described as single determinant (MO-like) to one that is a multideterminant (VB-like). The (9, 9)CAS for H atom addition was composed of the π and π^* orbitals of the benzyne ring, the symmetric and antisymmetric combination of the in-plane p atomic orbitals of the radical carbon centers, and the s orbital of hydrogen. A similar (10, 10) active space was utilized for H atom abstraction from CH_4, where the s orbital of hydrogen was replaced with the σ and σ^* orbitals of a C−H bond in methane. Geometry optimizations were performed at 25 fixed benzyne radical carbon (C1)-to-H atom substrate distances r_{C1-H} and 25 fixed r_{H3C-H} to yield a total of 50 points on the PES. The starting geometry aligned the substrate H atom along the axis of the phenyl radical product C1−H bond; however, this symmetry was not constrained. Complete geometry optimizations were performed at the energetic minima and maxima. Transition states were characterized by a single imaginary vibration corresponding to the reaction coordinate, and IRC analysis connected the TS to the reactant and product. Geometry optimizations of benzene with a (6, 6)CASSCF wave function (active space composed of the π and π^* electrons and orbitals) and the phenyl radical with a (7, 7)CASSCF wave function (active space composed of π and π^* electrons and orbitals and the radical electron and orbital) were also performed.

Each CASSCF wave function, including the (8, 8)CAS of the previously published benzyne isomers,[6] was subjected to local spin analysis using MELD.[14] The atomic volumes used in the projection operators were defined by partitioning space so that a point r is assigned to volume A if the distance of the point from A divided by the atomic radius of A is less than this ratio for any other atom. We have used atomic radii similar to those of Clementi et al.[15] for neutral atoms (C: 0.67 Å, H: 0.44 Å). The actual integrals are computed numerically using the same grid and weights as defined in Gaussian 98.[16] The atomic volumes defined in this way closely resemble the Bader atomic volumes[17,18] and result in charges that are similar to those given by Bader's atoms in molecules method but are easier to determine.

Theoretical Considerations

The previous derivation of local spin operators may be summarized as follows. The total spin operator for the electrons of a molecule is

$$\boldsymbol{S} = \sum_{i=1}^{N} \boldsymbol{S}(i) \tag{1}$$

where the sum is over all electrons. Hermitian one-electron position−space projection operators, P_A, are defined and associated with atomic centers (or larger fragments) within a molecule such that

$$P_A P_B = \delta_{AB} P_A \tag{2}$$

and

$$\sum_A P_A = 1 \tag{3}$$

The projection operators used here are based on atomic volumes and utilize the function $w_A(r)$ that is defined to be 1 for r in the volume associated with atom A and 0 otherwise. The total spin $\boldsymbol{S}$ is then

$$\boldsymbol{S} = \sum_A \boldsymbol{S}_A \tag{4}$$

where

$$\boldsymbol{S}_A = \sum_{i=1}^{N} \boldsymbol{S}(i) P_A(i) \tag{5}$$

The operator $\boldsymbol{S}_A$ defined in this way obeys the general definition of an angular momentum operator. Also,

$$\boldsymbol{S}^2 = \sum_A \sum_B \boldsymbol{S}_A \cdot \boldsymbol{S}_B \tag{6}$$

and

$$\boldsymbol{S}_A \cdot \boldsymbol{S}_B = {}^3/_4 \delta_{AB} \sum_{i=1}^{N} P_A(i) + \sum_{i>j} \boldsymbol{S}(i) \cdot \boldsymbol{S}(j) [P_A(i) P_B(j) + P_B(i) P_A(j)] \tag{7}$$

In the context of the Wiberg−Mayer definition of bond order (B_{AB}),[19] the average of $\boldsymbol{S}_{zA}$ for each center (m_A), and the intrinsic delocalization of the unpaired electron density (U_{AB})[1] for $A \neq B$, the average of eq 7 for a single Slater determinant wave function gives

$$\langle \boldsymbol{S}_A \cdot \boldsymbol{S}_B \rangle = -{}^3/_8 B_{AB} + m_A m_B + {}^1/_2 U_{AB} \tag{8}$$

For a single center, eq 7 becomes

$$\langle \boldsymbol{S}_A{}^2 \rangle = {}^3/_8 \sum_{B \neq A} B_{AB} + m_A{}^2 + {}^1/_2 F_A \tag{9}$$

where F_A is Mayer's definition of free valence[19] (the total valence of A minus the total B_{AB} to A). Programs to evaluate eqs 8 and 9 (for a single-determinant wave function) and the

analogous equations for a multideterminant wave function have been incorporated into MELD.[14]

This methodology, like any partitioning of a molecule into fragments, is somewhat arbitrary, and local spin operators experience some of the difficulties associated with any fragment population analysis. We have shown previously[1] that the partitioning scheme has a significant effect on the calculated charge about each center, whereas $\langle \boldsymbol{S}_A^2 \rangle$ and $\langle \boldsymbol{S}_A \cdot \boldsymbol{S}_B \rangle$ exhibit much less dependence. In the single-determinant approximation, m_A, F_A, and U_{AB} in eqs 8 and 9 may change slightly for different population analyses, yet these differences cancel in the computed values of $\langle \boldsymbol{S}_A^2 \rangle$ and $\langle \boldsymbol{S}_A \cdot \boldsymbol{S}_B \rangle$. Similar results have been observed for multideterminant wave functions. For example, in the full configuration interaction approximation of the H_2 dissocation PES, the spin properties obtained with Löwdin projection operators are nearly equivalent to those obtained by projectors based on atomic volumes. Indeed, significant differences in the spin properties were observed only at extremely small internuclear separations, where Löwdin population analysis is known to break down.

Results and Discussion

Local Spin Analysis of Benzyne. The local spin properties of benzyne are best understood after a brief description of these quantities for benzene (Table 1). Here, $\langle \boldsymbol{S}_A^2 \rangle$ values are on the diagonal elements of Table 1, whereas $\langle \boldsymbol{S}_A \cdot \boldsymbol{S}_B \rangle$ values are on the off-diagonal. In the single-determinant MO description of benzene, the value of $\langle \boldsymbol{S}_A^2 \rangle$ is $^3/_8$ of the total number of bonds to A, and $\langle \boldsymbol{S}_A \cdot \boldsymbol{S}_B \rangle$ is $-^3/_8$ of the bond order between A and B (eqs 8 and 9). These definitions utilize the Wiberg−Mayer bond order[19] (WMBO) that is given by the sum of the diagonal elements of $\Pi_{AB}\Pi_{BA}$, where Π_{AB} is the charge density matrix (Π) between centers A and B. Understanding the characteristics of this particular definition of bond order is important in the scientific community because it has gained wide acceptance through its implementation in Gaussian 98.[16] Because the WMBO is analogous to the square of the Hückel BO (HBO), it may be unnaturally small if the HBO is less than 1. Also, the WMBO cannot be used to discern between bonding and antibonding interactions because the sign of the coefficients in Π is lost in taking $\Pi_{AB}\Pi_{BA}$.

In the Hückel description of benzene, the nearest-neighbor π bond order is $^2/_3$, whereas the 1−3 HBO is 0 and the 1−4 HBO is $-^1/_3$. The corresponding WMBO values for the π electrons are the squares of the HBO numbers: $^4/_9$, 0, and $^1/_9$, respectively. The CNDO2[20] description, which takes into account the σ bonding in benzene, predicts that each carbon participates in two C−C σ bonds (WMBO = 0.60), one C−H σ bond (WMBO = 0.77), two nearest-neighbor σ bonds (WMBO = 0.44), and one 1−4 π interaction (WMBO = 0.11). The 1−3 σ and π interactions are 0. Thus, $\langle \boldsymbol{S}_H^2 \rangle = 0.37$, $\langle \boldsymbol{S}_C^2 \rangle = 1.31$, $\langle \boldsymbol{S}_C \cdot \boldsymbol{S}_H \rangle = -0.29$, $\langle \boldsymbol{S}_{C1} \cdot \boldsymbol{S}_{C2} \rangle = -0.39$, $\langle \boldsymbol{S}_{C1} \cdot \boldsymbol{S}_{C3} \rangle = 0.00$, and $\langle \boldsymbol{S}_{C1} \cdot \boldsymbol{S}_{C4} \rangle = -0.04$. The CNDO2 atomic orbitals are generally considered to be most similar to Löwdin orbitals, and similar local spin values would be expected using a Löwdin population analysis.[21] Here we utilize a Bader population analysis because our previous studies have shown that it is consistent for the widest variety of systems, including those with transition-metal centers. Bader analysis, using the Hartree−Fock wave function,[22] increases the total C1−C2 WMBO to 1.41. In turn, this trend causes spin expectation values that are larger in magnitude than the analogous CNDO2 results: $\langle \boldsymbol{S}_H^2 \rangle = 0.38$, $\langle \boldsymbol{S}_C^2 \rangle = 1.35$, $\langle \boldsymbol{S}_C \cdot \boldsymbol{S}_H \rangle = -0.35$, $\langle \boldsymbol{S}_{C1} \cdot \boldsymbol{S}_{C2} \rangle = -0.53$, $\langle \boldsymbol{S}_{C1} \cdot \boldsymbol{S}_{C3} \rangle = -0.03$, and $\langle \boldsymbol{S}_{C1} \cdot \boldsymbol{S}_{C4} \rangle = -0.04$. The use of a multideterminant wave function [(6, 6)CAS] yields spin quantities that are slightly larger because the π electrons have more VB character than they do in a single-determinant wave function: $\langle \boldsymbol{S}_C^2 \rangle = 1.63$, $\langle \boldsymbol{S}_{C1} \cdot \boldsymbol{S}_{C2} \rangle = -0.59$, $\langle \boldsymbol{S}_{C1} \cdot \boldsymbol{S}_{C3} \rangle = 0.01$, and $\langle \boldsymbol{S}_{C1} \cdot \boldsymbol{S}_{C4} \rangle = -0.08$.

TABLE 1: $\langle \boldsymbol{S}_A \cdot \boldsymbol{S}_B \rangle$ (Off-Diagonal Elements) and $\langle \boldsymbol{S}_A^2 \rangle$ (Diagonal Elements) Obtained from the (6, 6)CASSCF Wave Function of Benzene, the (7, 7)CASSCF Wave Function of the Phenyl Radical, and the (8, 8)CASSCF Wave Function of *o*-, *m*-, and *p*-Benzyne[6]

	benzene	C(1)	C(2)	C(3)	C(4)	C(5)	C(6)
	C(1)	1.63					
	C(2)	−0.59	1.63				
	C(3)	0.01	−0.59	1.63			
	C(4)	−0.08	0.01	−0.59	1.63		
	C(5)	0.01	−0.08	0.01	−0.59	1.63	
	C(6)	−0.59	0.01	−0.08	0.01	−0.59	1.63
	phenyl radical						
	C(1)	1.99					
	C(2)	−0.61	1.62				
	C(3)	0.03	−0.59	1.63			
	C(4)	−0.10	0.01	−0.59	1.63		
	C(5)	0.03	−0.08	0.01	−0.59	1.63	
	C(6)	−0.61	0.01	−0.08	0.01	−0.59	1.62
	o-benzyne						
	C(1)	1.80					
	C(2)	−1.16	1.80				
	C(3)	0.00	−0.53	1.62			
	C(4)	−0.08	0.01	−0.63	1.63		
	C(5)	0.01	−0.08	0.01	−0.55	1.63	
	C(6)	−0.53	0.00	−0.09	0.01	−0.63	1.62
	m-benzyne						
	C(1)	1.82					
	C(2)	−0.60	1.61				
	C(3)	−0.50	−0.60	1.82			
	C(4)	−0.09	0.01	−0.59	1.62		
	C(5)	0.00	−0.08	0.00	−0.58	1.62	
	C(6)	−0.59	0.01	−0.09	0.01	−0.58	1.62
	p-benzyne						
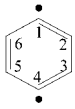	C(1)	2.01					
	C(2)	−0.63	1.62				
	C(3)	0.03	−0.58	1.62			
	C(4)	−0.76	0.03	−0.63	2.01		
	C(5)	0.03	−0.08	0.03	−0.63	1.62	
	C(6)	−0.63	0.03	−0.08	0.03	−0.58	1.62

Removal of a single hydrogen atom to generate the phenyl radical increases $\langle \boldsymbol{S}_C^2 \rangle$ at the radical center because the free-spin contribution to $\langle \boldsymbol{S}_C^2 \rangle$ ($\sim^3/_4$) is larger than is the C−H bond-order term ($\sim^3/_8$) in eq 9. Here the single- and multideterminant wave functions yield approximately the same result. Although one C−H bond no longer contributes to the $\langle \boldsymbol{S}_C^2 \rangle$ of the radical center, the unpaired electron now contributes its $\boldsymbol{S}^2$ to $\langle \boldsymbol{S}_C^2 \rangle$. Thus, the [(7, 7)CASSCF] $\langle \boldsymbol{S}_C^2 \rangle$ is 1.99 (Table 1). Nearest-neighbor spin-coupling values and the 1−4 coupling are observed to change slightly upon generation of the phenyl radical from benzene. The ROHF results for the phenyl radical are almost equivalent and have been reported previously.[1]

Removal of a second hydrogen at the ortho position results in significant localization of the C1−C2, C3−C4, and C5−C6 π bonds (Table 1) and subsequent distortion of the benzyne ring by a decrease in the C1−C2 inter-radical distance to 1.26 Å. Concurrent to the geometric distortion is a significant decrease in $\langle \boldsymbol{S}_{C1} \cdot \boldsymbol{S}_{C2} \rangle$ from −0.61 in the phenyl radical to −1.16. A pure triple bond in the single-determinant MO approximation

would have this value to be $-^3/_8\sum B_{AB}$, which is $-^3/_8(1 + 1 + 1)$ or -1.13 (eq 8). In contrast, a noninteracting but spin-coupled radical pair with a CASSCF wave function that resembles the purely covalent Heitler−London VB description[23] would have a coupling of $-^3/_4$ that when added to the sum of the remaining bond orders [$-^3/_8\sum B_{AB} = -^3/_8(1 + 1)$] would lead to a predicted value of -1.50. If one were to examine only $\langle \boldsymbol{S}_{C1}\cdot\boldsymbol{S}_{C2}\rangle$, it would be easy to conclude that *o*-benzyne is a triple-bonded species. Although the observed $\langle \boldsymbol{S}_{C1}^2\rangle$ and $\langle \boldsymbol{S}_{C2}^2\rangle$ [$\langle \boldsymbol{S}_{C1}^2\rangle = \langle \boldsymbol{S}_{C2}^2\rangle = 1.80$] values are much smaller than the value for the radical carbon in the phenyl radical, they are still much larger than the predicted values for a purely triple-bonded species that would have $\langle \boldsymbol{S}_{C1}^2\rangle$ equal to $\langle \boldsymbol{S}_{C2}^2\rangle$ with a value of 1.50.

The intermediacy of the $\langle \boldsymbol{S}_{C}^2\rangle$ values of the radical centers, in addition to the large spin coupling between C1 and C2, indicates that the triply bonded resonance structure is stabilized relative to the noninteracting diradical form such that the C1−C2 bond order is ∼2.5. This value is in good agreement with the current chemical consensus on this matter.[24−26] If the contribution to $\langle \boldsymbol{S}_{C1}\cdot\boldsymbol{S}_{C2}\rangle$ by a pure σ and an out-of-plane π bond is ignored, then the approximate $\langle \boldsymbol{S}_{C1}\cdot\boldsymbol{S}_{C2}\rangle$ coupling is only -0.38. Thus, the bonding character between C1 and C2 decreases the magnitude of $\langle \boldsymbol{S}_{C1}\cdot\boldsymbol{S}_{C2}\rangle$ relative to that predicted for a simple radical pair, or, in other words, the ionic portion of the MO approximation decreases what would be normally predicted by a purely covalent Heitler−London VB description. The large participation of the triply bonded resonance structure is also indicated by a heightened π contribution to the C3−C4 and C5−C6 bonds, which causes more negative $\langle \boldsymbol{S}_{C3}\cdot\boldsymbol{S}_{C4}\rangle$ and $\langle \boldsymbol{S}_{C5}\cdot\boldsymbol{S}_{C6}\rangle$ values relative to that of benzene. Also, the C1−C6, C2−C3, and C4−C5 bonds have a smaller π contribution than in benzene and, consequently, less negative $\langle \boldsymbol{S}_{C}\cdot\boldsymbol{S}_{C}\rangle$ values. The exceptionally high singlet−triplet gap (experimental ΔE_{ST} = 37.5 kcal/mol,[27] (8, 8) CASSCF/6-31G* ΔE_{ST} = 49.4 kcal/mol[6]) and the small number of effectively unpaired electrons (N_D = 0.77)[6] for this benzyne isomer support these conclusions.

The extent of open-shell character in *m*-benzyne has been under debate for some time in the literature. Generally, it is considered to have slightly more open-shell character than the ortho isomer, but it too has been previously described as intermediate between a pure diradical and a closed-shell (bicyclic) molecule.[27] The through-space bonding interaction between the radical centers leads to distortion of the ring and an inter-radical (8, 8)CASSCF C1−C3 distance of 2.20 Å.[6] Analysis of this wave function reveals a strong antiferromagnetic interaction between C1 and C3 [$\langle \boldsymbol{S}_{C1}\cdot\boldsymbol{S}_{C3}\rangle = -0.50$] (Table 1), which may be decomposed predominantly into an in-plane antiferromagnetic contribution and a small out-of-plane π ferromagnetic contribution. The C1−C3 spin interaction should be close to $-^3/_8$ if the electronic structure strongly resembles the closed-shell bicyclic molecule; however, $-^3/_4$ should result from two noninteracting but spin-coupled radicals. Therefore, the bicyclic resonance form contributes slightly more to the electronic structure than does the open-shell diradical form. Similar $\langle \boldsymbol{S}_{A}\cdot\boldsymbol{S}_{B}\rangle$ values between nearest-neighbor centers are observed, which indicates that *m*-benzyne exhibits minimal π localization. Interestingly, the spin expectation value at the radical centers is nearly equal to that found in *o*-benzyne; $\langle \boldsymbol{S}_{C1}^2\rangle$ equals $\langle \boldsymbol{S}_{C3}^2\rangle$ with a value of 1.82. Taking into account all of these results, we are led to the conclusion that this isomer is slightly more similar to *o*-benzyne than to *p*-benzyne. Indeed, the singlet−triplet gap (experimental ΔE_{ST} = 21.0,[26] (8, 8)-CASSCF/6-31G* ΔE_{ST} = 21.3[6]) and the number of effectively unpaired electrons (N_D = 1.38)[6] would place *m*-benzyne nearly intermediate between *o*- and *p*-benzynes.

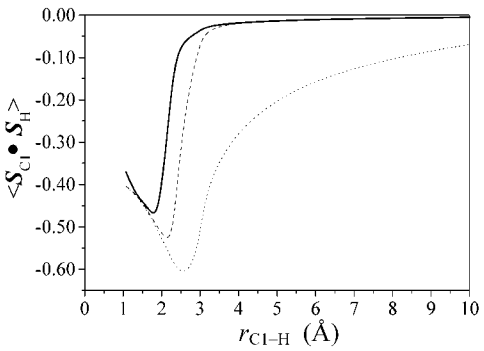

Figure 1. Plots of $\langle \boldsymbol{S}_{C1}\cdot\boldsymbol{S}_{H}\rangle$ between the diradical center C1 and the H atom in *o*- (—), *m*- (- - -), and *p*-benzyne (· · ·) along the H atom addition PES using the (9, 9)CASSCF/6-31G* wave function.

The last isomer, *p*-benzyne, has the most radical character and the least-distorted geometric structure [(8, 8)CASSCF inter-radical distance = 2.71 Å[6]] of all the benzyne isomers (experimental ΔE_{ST} = 3.8 kcal/mol,[27] (8, 8) CASSCF/6-31G* ΔE_{ST} = 2.9, and N_D = 1.94[6]). The spin expectation value for each radical center [$\langle \boldsymbol{S}_{C1}^2\rangle = \langle \boldsymbol{S}_{C4}^2\rangle = 2.01$] is nearly equal to that found in the phenyl radical. The spin coupling between these centers is also close to what is expected for two noninteracting but spin-coupled radicals that are well described by the Heitler−London VB model [$\langle \boldsymbol{S}_{C1}\cdot\boldsymbol{S}_{C4}\rangle = -0.76$]. However, it is important to note that -0.08 of $\langle \boldsymbol{S}_{C1}\cdot\boldsymbol{S}_{C4}\rangle$ is due to the 1−4 π antiferromagnetic coupling that is present in benzene. Thus, $\langle \boldsymbol{S}_{C1}\cdot\boldsymbol{S}_{C4}\rangle$ is slightly less than the ideal value. Unlike *o*- and *m*-benzyne, through-space pathways do not stabilize the bonding combination of in-plane p atomic orbitals relative to the antibonding combination. Rather, Hoffmann, Imamura, and Hehre[28] have shown that the in-plane antibonding MO delocalizes into the σ* orbital of the side 2−3 and 5−6 bonds, thereby stabilizing it relative to the bonding combination. Similarly, the in-plane bonding MO interacts with the σ orbital of the 2−3 and 5−6 bonds, which is destabilizing. Several other through-bond pathways have been identified that utilize the apical 1−2, 3−4, 4−5, and 6−1 C−C bonds as well. The importance of the latter through-bond mechanisms may be significant because we observe $\langle \boldsymbol{S}_{A}\cdot\boldsymbol{S}_{B}\rangle$ values that are slightly larger between the apical C−C bonds than between the side C−C bonds [$\langle \boldsymbol{S}_{C1}\cdot\boldsymbol{S}_{C2}\rangle = \langle \boldsymbol{S}_{C1}\cdot\boldsymbol{S}_{C6}\rangle = \langle \boldsymbol{S}_{C3}\cdot\boldsymbol{S}_{C4}\rangle = \langle \boldsymbol{S}_{C4}\cdot\boldsymbol{S}_{C5}\rangle = -0.63$, $\langle \boldsymbol{S}_{C2}\cdot\boldsymbol{S}_{C3}\rangle = \langle \boldsymbol{S}_{C5}\cdot\boldsymbol{S}_{C6}\rangle = -0.58$].

H Atom Addition to Benzyne. Of the multiple reaction pathways available to benzyne, H atom addition will likely occur if the substrate C−H bond disassociates while the substrate is far from the radical center. For these activationless additions, the (9, 9)CAS calculations give the following exothermicities: ortho ΔH_{rxn} = −73.6 kcal/mol, meta ΔH_{rxn} = −85.4 kcal/mol, and para ΔH_{rxn} = −96.6 kcal/mol. These agree well with the experimental bond strengths of the C−H bond of the phenyl radical at the ortho, meta, and para positions.[27,29]

The previously reported electronic changes for addition to the dihydrogen diradical model system can be observed directly in the (9, 9)CASSCF wave function of the actual benzynes (Figure 1). Each of the three plots of $\langle \boldsymbol{S}_{C}\cdot\boldsymbol{S}_{C}\rangle$ between the diradical centers illustrates that during bond formation the diradical carbon centers become less antiferromagnetically coupled. This decrease occurs the earliest in the reaction coordinate for *p*-benzyne + H, followed by the addition to the meta and ortho isomers. The same trend is observed in our previous VB analysis, that is, benzyne isomers with small ΔE_{ST}

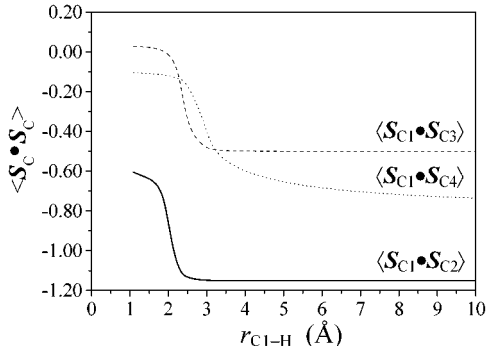

Figure 2. Plots of $\langle S_C \cdot S_C \rangle$ between the diradical centers in *o*- (—), *m*- (- - -), and *p*-benzyne (· · ·) along the H atom addition PES using the (9, 9)CASSCF/6-31G* wave function.

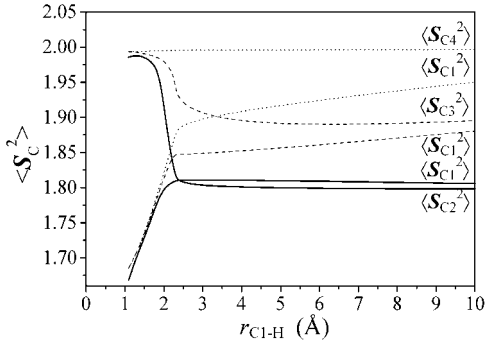

Figure 3. Plots of $\langle S_C^2 \rangle$ for each diradical center in *o*- (—), *m*- (- - -), and *p*-benzyne (· · ·) along the H atom addition PES using the (9, 9)CASSCF/6-31G* wave function.

values unpair the diradical electrons earlier in the reaction coordinate than do isomers with larger ΔE_{ST} values.

The magnitude of $\langle S_C \cdot S_C \rangle$ between the radical centers is inversely related to the spin coupling between the abstracting atom (C1 for each isomer) and the approaching H atom, $\langle S_{C1} \cdot S_H \rangle$, as seen in Figure 2. This Figure also clearly illustrates the strength of the perturbation caused by a nearby radical center on $\langle S_{C1} \cdot S_H \rangle$. In particular, C1 of *p*-benzyne is able to couple to the H atom the earliest in the reaction coordinate and with a value at the minimum $\langle S_{C1} \cdot S_H \rangle$ that is close to that expected for two noninteracting but spin-coupled radical centers. The proximity of the radical centers to each other is directly related to the magnitudes of $\langle S_{C1} \cdot S_{C3} \rangle$ and $\langle S_{C1} \cdot S_{C2} \rangle$ in *m*- and *o*-benzynes, leading to smaller values at the $\langle S_{C1} \cdot S_H \rangle$ minima that also occur later in the reaction coordinate. This behavior has mechanistic implications and could be considered to be one of the reasons that *p*-benzyne is known to perform "radical" chemistry, whereas other reaction pathways (e.g. electrophilic attack) are associated with *m*- and *o*-benzyne.

Plots of $\langle S_C^2 \rangle$ for the radical centers along the H atom addition reaction coordinate show that the local electronic structure of each site changes significantly during bond formation (Figure 3). Either bonding or antibonding interactions between the radical centers or between a radical center and another atom will decrease $\langle S_C^2 \rangle$ from the value of the phenyl radical. Thus, $\langle S_C^2 \rangle$ may be used as a measure of radical character at each site and potentially, of the reactivity. At the reactant portion of the PES, $\langle S_C^2 \rangle$ of the radical centers clearly shows increasing radical character in the order *o*- < *m*- < *p*-benzyne. According to chemical intuition, we expect and observe that $\langle S_{C1}^2 \rangle$ decreases during C1−H bond formation and that $\langle S_{C2}^2 \rangle$ (for *o*-benzyne), $\langle S_{C3}^2 \rangle$ (for *m*-benzyne), and $\langle S_{C4}^2 \rangle$ (for *p*-benzyne) increase to the value of the phenyl radical.

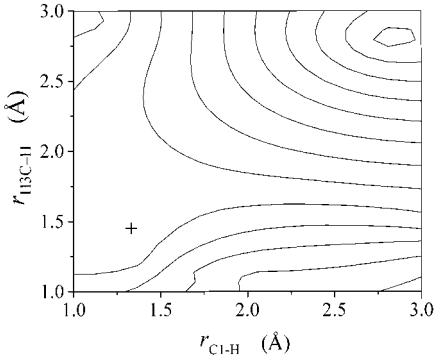

Figure 4. Two-dimensional plot of the *o*-benzyne abstraction from the CH_4 PES using a (10, 10)CASSCF/6-31G* wave function with the TS marked by a cross. The contour lines are shown every 0.006 au.

Interestingly, the slope for the decrease in $\langle S_{C1}^2 \rangle$ is the steepest for *p*-benzyne, followed by the slopes for the meta and ortho isomers. Similarly, the slope for the increase in $\langle S_{C2}^2 \rangle$, $\langle S_{C3}^2 \rangle$, and $\langle S_{C4}^2 \rangle$ follows the order *o*- > *m*- > *p*-benzyne. These observations agree nicely with the ability of each isomer to "unpair" its diradical electrons and subsequently facilitate bond formation. Also, one might expect in the case of *o*-benzyne + H that $\langle S_{C1}^2 \rangle$ might not change significantly if it is merely trading one in-plane C−C π bond for one C−H σ bond. The fact that $\langle S_{C1}^2 \rangle$ does decrease so dramatically further demonstrates the intermediacy of the strength of the in-plane C1−C2 π bond.

Benzyne H Atom Abstraction From CH_4. Unlike H atom addition, abstraction requires a large activation energy that arises from the unpairing of the C−H bonding electrons in CH_4. The relative magnitude of the calculated (10, 10)CAS $\Delta H^{\ddagger}$ follows the order of the experimental thermodynamic stability of the benzyne isomers: ortho $\Delta H^{\ddagger}$ = 34.9 kcal/mol, meta $\Delta H^{\ddagger}$ = 26.2 kcal/mol, and para $\Delta H^{\ddagger}$ = 19.6 kcal/mol. Similarly, the calculated ΔH_{rxn} values agree well with the observed order of increasing C−H bond strength in the phenyl radical at each position. It should be noted that the 6-31G* basis set is known to underestimate the C−H bond strength in methane because the (2, 2)CASSCF/6-31G* of CH_4 predicts that the C−H bond energy is 89.6 kcal/mol, whereas experimentally it is known to be 104.8 kcal/mol.[29] Nevertheless, for the purposes of wave function analysis, a correct C−H bond energy is not crucial.

The general shape of the abstraction PES for each of the benzyne isomers is reminiscent of the stretched H_2 + H_2 exchange reaction. For example, Figure 4 plots the 2D PES for *o*-benzyne abstraction from CH_4. The most significant difference in the shape of the PES between the three isomers is the location of the TS. The *o*-benzyne abstraction TS is located at r_{C1-H} equal to 1.28 Å and r_{H3C-H} equal to 1.48 Å, whereas in the *m*-benzyne reaction, the TS occurs earlier in the reaction coordinate at r_{C1-H} equal to 1.34 Å and r_{H3C-H} equal to 1.40 Å, and the TS for abstraction by the para isomer occurs earliest in the reaction at r_{C1-H} equal to 1.35 Å and r_{H3C-H} equal to 1.38 Å. This last TS occurs later in the reaction coordinate than that for the corresponding reaction using methanol instead of methane, as has been reported previously using a (4, 4)CASSCF wave function,[30] because of the difference in the exothermicities of the two reactions.

Because these PES clearly depend on two variables, so do the spin molecular properties, yet many of the general 1D trends in spin expectation values that were observed in the addition reaction are still valid during abstraction. First, we observe that the 1D slices through the 3D plots of $\langle S_C^2 \rangle$ for the benzyne radical centers along the reaction coordinate are comparable to

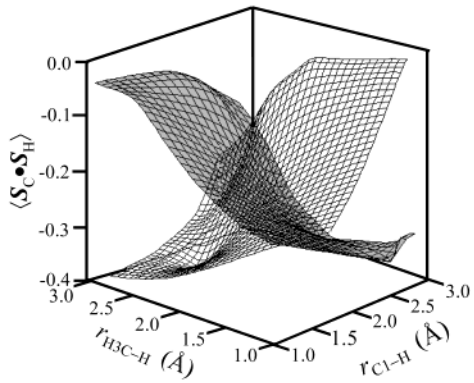

Figure 5. Three-dimensional plot of $\langle \boldsymbol{S}_{C1} \cdot \boldsymbol{S}_H \rangle$ (gray) and $\langle \boldsymbol{S}_C \cdot \boldsymbol{S}_H \rangle$ (transparent) between the methyl C and H atoms during the H abstraction by *o*-benzyne from CH_4 using a (10, 10)CASSCF/6-31G* wave function.

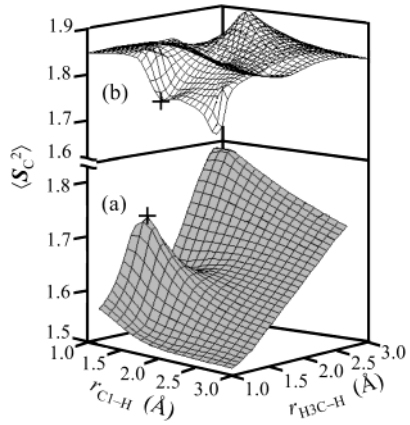

Figure 6. Three-dimensional plot of (a) $\langle \boldsymbol{S}_C^2 \rangle$ of the methyl moiety and (b) $\langle \boldsymbol{S}_C^2 \rangle$ of the abstracting radical center C1 during the H abstraction by *o*-benzyne from CH_4 using a (10, 10)CASSCF/6-31G* wave function. The TS is marked by a cross.

those of Figure 3. Similarly, the slices through the 3D plots of $\langle \boldsymbol{S}_C \cdot \boldsymbol{S}_C \rangle$ between the radical centers of each isomer yield the same information as does Figure 1. Second, we observe that the general shape of the 3D surface for $\langle \boldsymbol{S}_A \cdot \boldsymbol{S}_B \rangle$ between two centers that are involved in bond formation is nearly the inverse of the analogous dissociation surface. In particular, for *o*-benzyne abstraction, Figure 5 plots the 3D $\langle \boldsymbol{S}_{C1} \cdot \boldsymbol{S}_H \rangle$ surface (gray) on the same graph as the 3D $\langle \boldsymbol{S}_C \cdot \boldsymbol{S}_H \rangle$ surface (transparent) for the methyl carbon and disassociating H atom. As expected, the $\langle \boldsymbol{S}_{C1} \cdot \boldsymbol{S}_H \rangle$ maximum value occurs near the optimum r_{C1-H} and infinite r_{H3C-H}, whereas the minimum occurs at infinite r_{C1-H} and the optimum r_{H3C-H}. The reverse is true for the trend in $\langle \boldsymbol{S}_C \cdot \boldsymbol{S}_H \rangle$ values between the methyl carbon and H atom.

One may similarly monitor the $\langle \boldsymbol{S}_C^2 \rangle$ of the methyl carbon and the abstracting radical center to investigate the relationship between spin expectation values and radical character, as shown in Figure 6. Here, the lower surface (Figure 6a) represents $\langle \boldsymbol{S}_C^2 \rangle$ for the methyl carbon, and the upper surface (Figure 6b) illustrates the $\langle \boldsymbol{S}_{C1}^2 \rangle$ surface of *o*-benzyne (the abstracting radical center).

At the beginning of the reaction coordinate, the H_3C-H bond is fully formed, and Figure 6a shows that $\langle \boldsymbol{S}_C^2 \rangle$ of the methyl carbon is nearly the $^3/_8$ of the sum of all its bonds because the single-determinant approximation is valid for CH_4 [(10, 10)-CASSCF $\langle \boldsymbol{S}_C^2 \rangle = 1.52$]. At this coordinate in Figure 6b, $\langle \boldsymbol{S}_{C1}^2 \rangle$ is nearly unperturbed from free *o*-benzyne and is at the global maximum on its surface: $\langle \boldsymbol{S}_{C1}^2 \rangle = 1.85$. As the TS is approached, the methyl $\langle \boldsymbol{S}_C^2 \rangle$ increases because the $-^3/_8 \Sigma B_{AB}$ contribution of the H_3C-H bond to $\langle \boldsymbol{S}_C^2 \rangle$ is diminishing, whereas $\langle \boldsymbol{S}_{C1}^2 \rangle$ of *o*-benzyne decreases because of the increased C1−H bonding interaction. At the TS, a local maximum is observed in the methyl $\langle \boldsymbol{S}_C^2 \rangle$, and a local minimum is observed in $\langle \boldsymbol{S}_{C1}^2 \rangle$ of *o*-benzyne. Interestingly, proceeding along r_{H3C-H} from the TS yields another local minimum on the methyl $\langle \boldsymbol{S}_C^2 \rangle$ surface that is the result of the singlet coupling of the methyl radical carbon product to the phenyl radical carbon with a $\langle \boldsymbol{S}_A \cdot \boldsymbol{S}_B \rangle$ value of approximately $-^3/_8$ (Figure 7). Therefore, at this point, the wave function is best described by a delocalized MO over both centers. As r_{H3C-H} increases to infinity, this $\langle \boldsymbol{S}_A \cdot \boldsymbol{S}_B \rangle$ goes to $-^3/_4$, as expected for two well-separated and localized radical centers coupled as a singlet. The abstraction product is characterized by a global minimum in $\langle \boldsymbol{S}_{C1}^2 \rangle$ of the phenyl radical that is caused by the $-^3/_8$ contribution of the C1−H bond to $\langle \boldsymbol{S}_{C1}^2 \rangle$ in the single-determinant approximation. Analogously, $\langle \boldsymbol{S}_C^2 \rangle$ of the methyl carbon is a global maximum because of the $+^3/_8$ contribution of the localized, singly occupied orbital in eq 9.

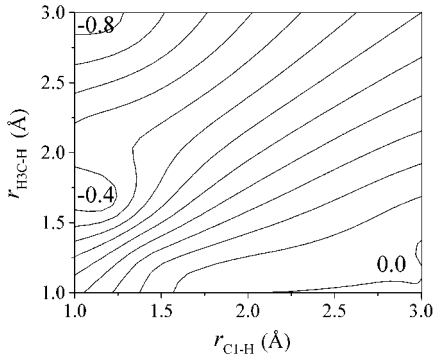

Figure 7. Two-dimensional plot of $\langle \boldsymbol{S}_C \cdot \boldsymbol{S}_C \rangle$ between the methyl carbon and C6 of *o*-benzyne during the H abstraction from CH_4 using a (10, 10)CASSCF/6-31G* wave function. The lowest contour is at −0.8, and the highest contour is at 0.0. The contour lines are shown every 0.07 au.

Conclusions

Although one typically associates spin properties with magnetic molecules, these local spin operators yield nonzero, chemically relevant quantities regardless of whether the molecule is closed or open shell. Here we have shown that these operators are sensitive to changes in the wave function and thus the electronic structure of a system. In the single-determinant MO approximation, the expectation values of the operators are chemically intuitive once the terms in eqs 8 and 9 are understood. However, their values are also capable of standing alone when the mathematical relationships in eqs 8 and 9 are no longer valid, as in multideterminant wave functions. There, bond order and free valence are technically not defined. In this instance, $\langle \boldsymbol{S}_A^2 \rangle$ and $\langle \boldsymbol{S}_A \cdot \boldsymbol{S}_B \rangle$ still yield chemically intuitive results and complement the known changes in a wave function along a reaction coordinate or between a series of molecules. $\langle \boldsymbol{S}_A^2 \rangle$ and $\langle \boldsymbol{S}_A \cdot \boldsymbol{S}_B \rangle$ are particularly useful in understanding changes in bonding and the development of radical character on atoms. Moreover, they are fairly unique because they are "atom-centered" or "molecular fragment-centered" properties. This partitioning is advantageous because it allows the direct comparison of a quantity for the purpose of studying reactivity.

Importantly, this method does require qualitatively correct wave functions to obtain reasonable results. For example, the broken symmetry/broken spin UHF or UDFT treatment of the

benzyne diradicals may give reasonable energies, but because these wave functions are not spin eigenfunctions, their spin properties cannot be expected to be correct. However, one could use these spin operators to quantify the differences between multi- and single-determinant wave functions for a given system. For example, our experiences with the DFT, UHF, and CASSCF descriptions of *p*-benzyne indicate that $\langle \boldsymbol{S}_A^2 \rangle$ and $\langle \boldsymbol{S}_A \cdot \boldsymbol{S}_B \rangle$ differ significantly only if *A* or *B* is one of the radical centers. This indicates that the other atoms and bonds in *p*-benzyne are fairly well described by a single-determinant description, a conclusion that is in good agreement with previous studies.

Acknowledgment. This work was supported by grant no. CHE-9982415 from the National Science Foundation. We also thank Professor Jeffrey Zaleski for thoughtful discussions regarding this manuscript.

References and Notes

(1) Clark, A. E.; Davidson, E. R. *J. Chem. Phys*. **2001**, *115*, 7382. Davidson, E. R.; Clark, A. E. *J. Mol. Phys*. **2002**, *100*, 373.

(2) See for example Wittig, G. *Naturwissenschaften* **1942**, *30*, 696. Roberts, J. D.; Simmons, H. E.; Carlsmith, L. A.; Vaughan, C. W. *J. Am. Chem. Soc.* **1953**, *75*, 3290. Wittig, G. *Angew. Chem.* **1965**, *77*, 752. Brown, A. T.; Christopher, T. A.; Levin, R. H. *Tetrahedron Lett.* **1976**, *46*, 4111. Miller, R. G.; Stiles, M. *J. Am. Chem. Soc.* **1963**, *85*, 1798. Nunn, E. *Tetrahedron Lett.* **1976**, *46*, 4199.

(3) See for example Sander, W. *Acc. Chem. Res.* **1999**, *32*, 669. Nelson, E. D.; Artau, A.; Price, J. M.; Kenttämaa, H. I. *J. Am. Chem. Soc.* **2000**, *122*, 8781. Thoen, K. K.; Kenttämaa, H. I. *J. Am. Chem. Soc.* **1999**, *121*, 800. Kraka, E.; Cremer, D.; Bucher, G.; Wandel, H.; Sander, W. *Chem. Phys. Lett.* **1997**, *268*, 313.

(4) See for example *Enediyne Antibiotics as Antitumor Agents*; Borders, D. B., Doyle, T. W., Eds.; Marcel Dekker: New York, 1995. Kaneko, T.; Takahashi, M.; Hirama, M. *Tetrahedron Lett.* **1999**, *40*, 2015. Jones, G. B.; Plourde, G. W., II; Wright, J. M. *Org. Lett.* **2000**, *2*, 811. Dai, W.-M.; Fong, K. C.; Lau, C. W.; Zhou, L.; Hamaguchi, W.; Nishimoto, S. *J. Org. Chem.* **1999**, *64*, 682. Konig, B.; Pitsch, W.; Thondorf, I. *J. Org. Chem.* **1999**, *61*, 4258. Nicolaou, K. C.; Dai, W. -M.; Hong, Y. -P.; Tsay, S.-C.; Baldridge, K. K.; Seigel, J. S. *J. Am. Chem. Soc.* **1993**, *115*, 7944. Nicolaou, K. C.; Liu, A.; Zeng, Z.; McComb, S. *J. Am. Chem. Soc.* **1992**, *114*, 9279. Nicolaou, K. C.; Hong, Y.-P.; Torisawa, Y.; Tsay, S. -C.; Dai, W. -M. *J. Am. Chem. Soc.* **1991**, *113*, 9878. Magnus, P.; Fortt, S.; Pitterna, T.; Snyder, J. P. *J. Am. Chem. Soc.* **1990**, *112*, 4986. Nicolaou, K. C.; Owaga, Y.; Zuccarello, G.; Kataoka, H. *J. Am. Chem. Soc.* **1988**, *110*, 7247. Magnus, P.; Carter, P. A. *J. Am. Chem. Soc.* **1988**, *110*, 1626. Konishi, M.; Ohkuma, H.; Matsumoto, K.; Tsuno, T.; Kamei, H.; Miyaki, T.; Oki, T.; Kawaguchi, H.; VanDuyne, G. D.; Clardy, J. J. *Antibiotics* **1989**, *42*, 1449. Smith, A. L.; Nicolaou, K. C. *J. Med. Chem.* **1996**, *39*, 2103. Kraka, E.; Cremer, D. *J. Am. Chem. Soc.* **2000**, *122*, 8245.

(5) Zhang, X.; Chen, P. *J. Am. Chem. Soc.* **1992**, *114*, 3147.

(6) Clark, A. E.; Davidson, E. R. *J. Am. Chem. Soc.* **2001**, *123*, 10691.

(7) Takatsuka, K.; Fueno, T.; Yamaguchi, K. *Theor. Chim. Acta* **1978**, *48*, 175. Staroverov, V. N.; Davidson, E. R. *Chem. Phys. Lett*. **2000**, *330*, 161.

(8) Hegarty, D.; Robb, M. A. *Mol. Phys.* **1979**, *38*, 1795.

(9) Eade, R. H. A.; Robb, M. A. *Chem. Phys. Lett.* **1981**, *83*, 362.

(10) Schlegal, H. B.; Robb, M. A. *Chem. Phys. Lett.* **1982**, *93*, 43.

(11) Bernardi, F.; Bottine, A.; McDougall, J. J. W.; Robb, M. A.; Schlegal, H. B. *Faraday Symp. Chem. Soc.* **1984**, *19*, 137.

(12) Hehre, W. J.; Ditchfield, R.; Pople, J. A. *J. Chem. Phys.* **1972**, *56*, 2257. Hariharan, P. C.; Pople, J. A. *Theor. Chim. Acta* **1973**, *28*, 213.

(13) Dupuis, M.; Marquez, A.; Davidson, E. R. *HONDO 99.6*; IBM Corporation: Kingston, NY, 1999.

(14) MELD is a set of electronic structure codes written originally by L. E. McMurchie, S. T. Elbert, S. R. Langhoff, and E. R. Davidson with extensive modification by D. Feller and D. C. Rawlings.

(15) Clementi, E.; Raimondi, D. L.; Reinhardt, W. P. *J. Chem. Phys*. **1967**, *47*, 1300.

(16) Frisch, M. J.; Trucks, G. W.; Schlegel, H. B.; Scuseria, G. E.; Robb, M. A.; Cheeseman, J. R.; Zakrzewski, V. G.; Montgomery, J. A., Jr.; Stratmann, R. E.; Burant, J. C.; Dapprich, S.; Millam, J. M.; Daniels, A. D.; Kudin, K. N.; Strain, M. C.; Farkas, O.; Tomasi, J.; Barone, V.; Cossi, M.; Cammi, R.; Mennucci, B.; Pomelli, C.; Adamo, C.; Clifford, S.; Ochterski, J.; Petersson, G. A.; Ayala, P. Y.; Cui, Q.; Morokuma, K.; Malick, D. K.; Rabuck, A. D.; Raghavachari, K.; Foresman, J. B.; Cioslowski, J.; Ortiz, J. V.; Stefanov, B. B.; Liu, G.; Liashenko, A.; Piskorz, P.; Komaromi, I.; Gomperts, R.; Martin, R. L.; Fox, D. J.; Keith, T.; Al-Laham, M. A.; Peng, C. Y.; Nanayakkara, A.; Gonzalez, C.; Challacombe, M.; Gill, P. M. W.; Johnson, B. G.; Chen, W.; Wong, M. W.; Andres, J. L.; Head-Gordon, M.; Replogle, E. S.; Pople, J. A. *Gaussian 98*, revision A.7; Gaussian, Inc.: Pittsburgh, PA, 1998.

(17) Biegler, F. W.; Nguyen-Dang, T. T.; Tal, Y.; Bader, R. F. W.; Duke, A. J. *J. Phys. B: At. Mol. Opt. Phys.* **1981**, *14*, 2739.

(18) Bader, R. F. W. *Atoms in Molecules: A Quantum Theory*; Oxford University Press: Oxford, U.K., 1990.

(19) Mayer, I. *Int. J. Quantum Chem.* **1986**, *29*, 73. Mayer, I. *Int. J. Quantum Chem.* **1986**, *29*, 477.

(20) Pople, J. A.; Beveridge, D. L. *Approximate Molecular Orbital Theory*; McGraw-Hill: New York, 1970.

(21) Löwdin, P. O. *J. Chem. Phys.* **1950**, *18*, 365.

(22) At the optimized Hartree−Fock geometry and with the 6-31G* basis set.

(23) Heitler, W.; London, F. *Physik* **1927**, *44*, 455.

(24) Scheiner, A. C.; Schaefer, H. F., III. *Chem. Phys. Lett.* **1991**, *177*, 471.

(25) Radziszewski, J. G.; Hess, B. A., Jr.; Zahradnik, R. *J. Am. Chem. Soc.* **1992**, *114*, 52.

(26) Blucsky, O.; Spirko, V.; Kobayashi, R.; Jorgensen, P. *Chem. Phys. Lett.* **1994**, *228*, 568.

(27) Wenthold, P. G.; Squires, R. R.; Lineberger, W. C. *J. Am. Chem. Soc.* **1998**, *120*, 5279.

(28) Hoffmann, R.; Imamura, A.; Hehre, W. J. *J. Am. Chem. Soc.* **1968**, *90*, 1499.

(29) Chase, M. W., Jr. NIST−JANAF Thermochemical Tables, 4th ed., *J. Phys. Chem. Ref. Data*, Monograph 9, **1998**, 1−1951.

(30) Logan, C. F.; Chen, P. *J. Am. Chem. Soc.* **1996**, *118*, 2113.